Journal of
Composites Science

MDPI

Article

Study on Machining Quality in Abrasive Water Jet Machining of Jute-Polymer Composite and Optimization of Process Parameters through Grey Relational Analysis

Murthy BRN [1], Rajendra Beedu [1], Jayashree P K [1,*] and Srinivasa Rao Potti [2]

[1] Department of Mechanical and Industrial Engineering, Manipal Institute of Technology, Manipal Academy of Higher Education, Manipal 576104, India; murthy.brn@manipal.edu (M.B.); rajbeedu60@gmail.com (R.B.)
[2] Department of Humanities and Management, Manipal Institute of Technology, Manipal Academy of Higher Education, Manipal 576104, India; srinivasa.potty@manipal.edu
* Correspondence: jayashree.pk@manipal.edu

Abstract: Abrasive Water Jet Machining (AWJM) is a popular machining method used to machine polymer matrix composites that are sensitive to temperature. This method is non-thermal, and each input parameter has a significant effect on output parameters, such as material removal rate, kerf width, surface roughness, and the potential for delamination. To ensure high-quality machining, it is crucial to set these input parameters at their optimal level. This paper proposes a simple approach to predict the optimum process parameters of water jet machining operations on jute fiber-reinforced polymer composite (JFRPC). The process parameters considered are standoff distance (SOD), traverse speed (TS), and abrasive material flow rate (MFR). Conversely, surface roughness (Ra) and delamination (Da) are the output parameters. Process parameters are set using Taguchi's L27 array, with consideration given to three levels of each input parameter. The best value for process parameters is found using grey relational analysis (GRA), and an ANOVA on GRA illustrates the impact of each input variable. After a confirmation test, it was found that the suggested parameters guarantee the best possible results.

Keywords: water jet machining (WJM); JFRP composite; orthogonal array; grey relational analysis

check for updates

Citation: BRN, M.; Beedu, R.; P K, J.; Potti, S.R. Study on Machining Quality in Abrasive Water Jet Machining of Jute-Polymer Composite and Optimization of Process Parameters through Grey Relational Analysis. *J. Compos. Sci.* **2024**, *8*, 20. https://doi.org/10.3390/jcs8010020

Academic Editor: Francesco Tornabene

Received: 21 November 2023
Revised: 18 December 2023
Accepted: 21 December 2023
Published: 8 January 2024

1. Introduction

AWJM is a non-traditional machining technique that is suitable for materials sensitive to temperature changes [1]. During AWJM, high-pressure water is mixed with sharp abrasive particles, which are then directed through a nozzle and onto the material's surface to be machined. The high-velocity abrasive particles erode the surface, causing material removal [2]. This method can be used to machine complex geometries with minimal distortion, stress, and heat-affected areas. Since no chemicals are used, AWJM is considered to be an environmentally friendly machining process.

The quality of AWJM (Abrasive Water Jet Machining) is evaluated based on several factors such as the kerf width, surface roughness, and delamination at the machined area. These factors are dependent on the process parameters of AWJM such as water pressure, abrasive feed and flow rate, type of abrasives used, and cutting parameters like standoff distance, impingement angle, and traverse speed. These process variables have a significant impact on the performance of AWJM [3]. Two wear zones are said to be present on AWJM machined surfaces [4]. The first is the cutting wear zone, which is created when abrasives impinge at sharp angles on the material surface and cut the material [5]. A second deformation wear zone is created when the abrasives hit the material surface at obtuse impact angles [6]. Large impact angles result in a deformed and rough machined surface, whereas smaller impact angles yield smooth cutting surfaces [7].

Optimizing the process parameters of Abrasive Water Jet Machining (AWJM) is crucial to guaranteeing damage-free machining, shorter production lead times, and reducing the rejection percentage. Process parameter optimization not only facilitates the production process but also lowers production costs. Many researchers have worked on optimizing the AWJM process for composite materials using various optimization methods. Among these, the Taguchi optimization technique is commonly utilized to process fiber-reinforced polymers (FRP) with the minimum number of experiments. According to Madival et al. [8], the traverse speed has the greatest influence on the top kerf width, bottom kerf width, and material removal rate, respectively. The effect of AWJM input parameters, such as transverse speed, standoff distance, and jet pressure, on the quality of the machined surface of SiC-filled polymer composite was investigated by Kavimani et al. [9] using the Taguchi coupled with grey relational analysis. They came to the conclusion that transverse speed and standoff distance parameters have a major influence. Thakur et al. [10] conducted a study to optimize the Abrasive Water Jet Machining (AWJM) parameters for machining carbon nanotube-filled epoxy/carbon composites. They used Taguchi design in conjunction with grey relational analysis and found that an increase in water jet pressure led to a decrease in delamination factor, surface roughness, and kerf width, while simultaneously increasing the material removal rate. They also concluded that the standoff distance was the least influential parameter that affected the machining quality. Chenrayan and his colleagues in their study [11] used the AWJM process to machine glass-carbon FRP. They applied a hybrid grey relational analysis and principal component analysis to minimize delamination and kerf taper. Their findings suggest that the water jet pressure is the most important component that may minimize the kerf angle. The standoff distance is the second most important factor, followed by the abrasive mass flow rate, in minimizing delamination. Their research aims to optimize the AWJ drilling parameters for carbon fiber-reinforced composites with varying fiber orientation angles. Karataş et al. [12] conducted a study using Taguchi design and multi-objective optimization to determine the effects of the standoff distance and jet pressure on the kerf angle and roundness error. To optimize the AWJM process parameters for the machining of epoxy/glass fiber/grinding wheel particle composite, Gopal et al. [13] applied a multi-objective optimization technique to investigate the impact of different parameters on the machining result of composites. Their findings suggest that the amount of filler in the composite has a greater influence on the kerf angle and surface roughness. Moreover, they demonstrate that the parameter standoff distance is the most significant factor affecting the machining result. Tomasz Szatkiewicz and his colleagues applied AWJM on 3-D printed stainless steel–polymer composite and predicted the most influencing parameter on surface roughness through the S-N ratio [14]. Andrzej Perec et al. worked on AWJM of industrial phenolic composite and developed a cutting model through a second-degree multinomial equation. They used RSM to develop the cutting model to optimize the depth of cut [15]. In another work, the same authors, Andrzej Perec et al., applied this AWJM to machine Hardox® steel and optimized the process parameters to obtain a better kerf width, cutting depth, and roughness of the machined surface. For this optimization process, they used a multi-criteria optimization grey relational analysis method [16].

Research Motivation

In recent years, natural fibers derived from plants have become increasingly popular as a substitute for synthetic ones [17]. One such natural fiber that can be used to construct lightweight, biodegradable, and sustainable fiber-reinforced polymer (FRP) is jute fiber [18]. It is important to note that the final property of the FRP depends on the orientation of the fibers within the laminates and the type of fibers used as reinforcements [19]. While the mechanical characteristics of jute-reinforced FRP are similar to those of FRP reinforced with synthetic fibers, the flammability of jute fibers makes machining jute-reinforced FRP more difficult [20]. Therefore, machining parameter optimization is crucial for jute/epoxy FRP. Although there are some papers available on the optimization of FRP, there is a limited number of research studies focusing on the optimization of machining parameters for jute-reinforced FRP using the grey relational analysis method. This study aims to prepare jute fiber-reinforced epoxy composites and machine these composites with an optimized AWJM process to obtain the minimum surface roughness and delamination, bridging the research gap and contributing to the current literature knowledge base.

2. Materials and Methods

2.1. The Materials Used

Fiber material: Jute is a natural fiber obtained from the Corchorus plant, which can grow up to almost 3 m tall. Jute fibers are mainly composed of two plant materials: lignin and cellulose. Lignin is a major component of wood fiber, while cellulose is an essential part of plant fiber. Jute is therefore a type of lignocellulosic fiber, containing a small amount of textile and wood components. The density of jute fiber ranges from 1.48 to 1.50 gm/cm^3, and it has a varying tenacity of 3.5–7 g/den, but is still quite strong. Jute fibers can appear in different colors, ranging from brown to yellow, depending on the growing environment. Under normal air conditions, the fiber breaking elongation is between 1.2 and 3.4 percent. Jute is not very flexible, but it is an excellent heat and electrical insulator.

Matrix material: In this work, general-purpose epoxy resin is used as the matrix material. Epoxy resins are known for their strength, adhesion, and resistance to moisture and chemicals, as well as their superior electrical and thermal insulation properties.

Curing of specimen: The process of curing composite materials is a crucial step in their production, as it transforms the basic components into a strong and durable structure. During the curing process, heat, pressure, and sometimes special chemicals are applied to give the final product the desired properties. In this particular project, K6 hardener is used. This hardener is a liquid that cures at room temperature and has low viscosity. It acts as a catalyst, helping the resin develop cross-links and cure at room temperature. It is commonly used in manual layup applications, and its high reactivity ensures quick curing at room temperature. Laminates produced using this hardener can withstand a temperature range of 20 °C to 100 °C. The curing process is carried out in heat-pressed mode.

Composite specimen preparation: A popular and simple manufacturing method for producing composites is the hand layup technique. The matrix material used in this method is a general-purpose polyester resin called bisphenol A (BPA), which is purchased from Renuka Enterprises, Mumbai, India. Huntsman Polymers is the manufacturer of this resin. K6 hardener is used in this preparation, with a 10% percentage of hardener. Before creating the composite specimens, jute fiber mats are cut to the required size and kept ready. Measurable amounts of resin and fiber mat are used to achieve the desired volume fraction. Jute fiber volume fraction is kept at 35% by weight, whereas epoxy volume is kept at 65% by weight.

To facilitate easy removal of the composite, the supporting plate is thoroughly cleaned and a releasing agent is applied. The first layer of fiber is placed on the plate, and resin is added. Once enough resin is added to impregnate the resin, a roller is used to remove trapped air from the mat. This stacking procedure is repeated until all the estimated fiber mat and resin are added, with a chosen inclination of 90° for the jute fiber. After stacking, the upper plate is placed in the vicinity, and the fiber and the resin are protected in a polythene cover. The complete assembly is positioned in a hot compression device for 48 h while maintaining a temperature of 60° and applying a force of 100 kg/mm^2 to remove trapped air and to cure. Once the curing is complete, the excess fibers are snipped off from all sides, and the composite specimen is taken. The hand layup method used is represented in Figure 1 schematically.

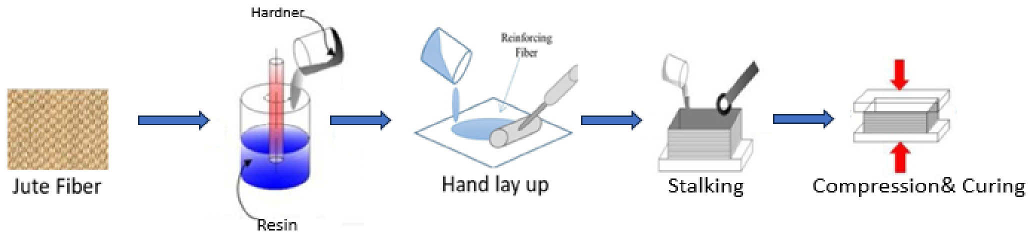

Figure 1. Schematic representation of the hand layup method used to produce the specimen.

2.2. Machining Process

The specimens were firmly fixed on cardboard by using double-sided sticky tape. The machining process was carried out using a 5-axis abrasive water jet cutting machine (Omax Corp. Kent WA, USA: model no. MAXIEM1515). There were three variable input parameters, which were standoff distance (SOD), traverse speed (TS), and abrasive mass flow rate (MFR). For each parameter, three levels of variation were chosen. The mass flow rates were 0.25, 0.3, and 0.35 kg/min; the traverse speed levels were 20, 25, and 30 mm/min; and the standoff distances were 2, 3, and 4 mm. The selected machining parameters were based on prior studies conducted by multiple researchers. They discovered that the range under consideration yields superior machining qualities on jute epoxy composites. To ensure accurate machining, the setup was tested for multiple parameters before beginning the machining process, even though the machine was regularly inspected and kept in good working order. It was verified through inspection that there was no wear or damage to the nozzle or orifice. To guarantee precision cuts, it was necessary to measure and modify the abrasive flow rate. The level of water pressure was tested and fixed. The traverse speed for each level was calculated and modified based on the desired outcome. Precision was used in the checking and setting of standoff distance values. The abrasive mixing ratios were meticulously monitored and adjusted to guarantee adequate mixing with water. The cutting depth was calibrated and adjusted to fit the test specimen to ensure precision cuts. Finally, test cuts were made to verify accurate cutting of the specimen once all parameters had been verified and set to the correct values.

Water jet machining was carried out in this experiment, using almandine garnet as the abrasive material. Almandine garnet is a well-known, affordable material that is popular for its sharp edges and hardness. This garnet is a class of closely related silicate minerals. A wide range of colors, including red, orange, yellow, green, purple, brown, blue, black, pink, and colorless, are frequently observed in garnets. Almandine is one of the most popular and well-known garnet kinds because of its distinctive deep red to reddish-brown color. The chemical formula of almandine is $Fe_3Al_2(SiO_4)_3$. Almandine can be found in some igneous rocks, as well as metamorphic rocks like gneiss and schist, and in placer deposits, where it has been concentrated in sedimentary contexts after weathering from its original source rocks. Almandine can effectively cut through metals, ceramics, and composite materials. On the Mohs hardness scale, almandine garnet is rated between 7.5 and 8.0. Various mesh sizes are available for this abrasive material, ranging from a very fine 230 mesh to a coarse 50 mesh. In this study, a mesh size of 80 was used. Mesh 80 garnet is the most commonly used and efficient abrasive for water jet machining. Unlike other abrasive materials, garnet is generally non-toxic and non-hazardous, making it less harmful to human health and the environment. The water jet pressure was kept constant at 200 MPa, and the jet angle was kept at 90° to the workpiece.

2.3. Machining Parameters Levels Selection

Standoff distance (SOD), traverse speed (TS), and abrasive material flow rate (MFR) are the chosen input parameters. Table 1 displays the three parameters along with their respective levels. A review of the literature is used to determine the machining parameters [21].

Table 1. Levels of process parameters.

Parameters	Traverse Speed (TS) (A)	Stand Off Distance (SOD) (B)	Material Flow Rate (MFR) (C)
Unit	mm/min	mm	kg/min
Level 1	20	2	0.25
Level 2	25	3	0.30
Level 3	30	4	0.35

2.4. Process Parameters Selection for Every Single Trial

For the present experimentation, the selection of the process parameters is made on the basis of Taguchi's L27 orthogonal array. With this array, the smallest number of experiments necessary to obtain a near-accurate solution is guaranteed. Measured and tabulated output parameters are produced. The output parameters are measured and tabulated. The surface roughness Ra is measured in µm, using Taylor Hobson Surtronic 3+ as shown in Figure 2a, and delamination was measured in mm^2 using ImageJ 1.52 software, as illustrated in Figure 2b. The Mitutoyo SJ 210 advanced surface roughness profilometer is highly functional. It is a premium quality instrument made by a Japanese company. This instrument is light, compact, and simple to operate, with efficient and convenient data management. The specifications of the instrument used are presented in Table 2. The sampling length taken is 2.5 mm. The L27 orthogonal array and corresponding response are shown in Table 3.

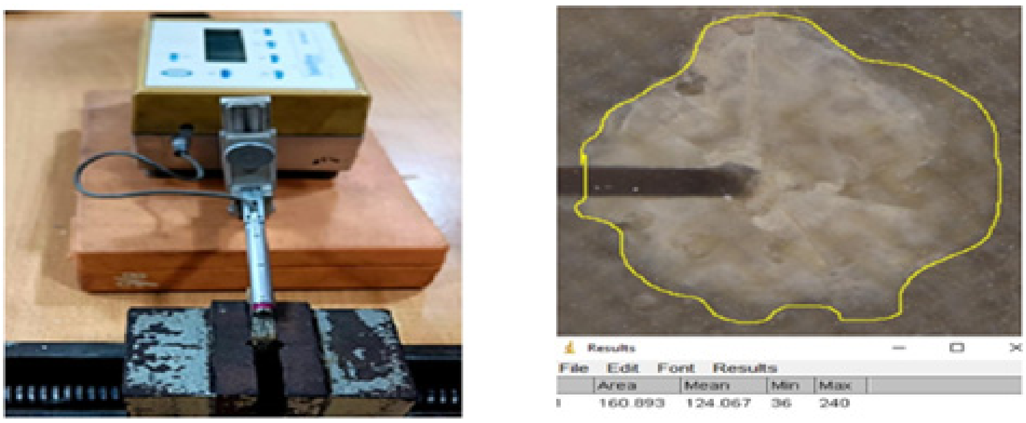

(**a**) (**b**)

Figure 2. Measurement of surface roughness (**a**) and measurement of delamination (**b**).

Table 2. Specifications of Mitutoyo SJ 210 surface roughness measurement instrument.

Standards	JIS 82/JIS 94/JIS 01/ISO 97/ANSI/VDA
Parameters	Ra, Rc, Ry, Rz, Rq, Rt, Rmax, Rp, Rv, R3z, Rsk, Rku, RPc, Rsm, Rz1max, S, HSC, RzJIS, Rppi, RΔa, RΔq, Rlr, Rmc, Rmr(c), Rk, Rpk, Rvk, Mr1, Mr2, A1, A2, Vo, Rpm, tp, Htp, R, Rx, AR
Filters	Gaussian, 2CR75, PC75
Cut-off length	0.08 mm, 0.25 mm, 0.8 mm, 2.5 mm
Sampling Length	0.08 mm, 0.25 mm, 0.8 mm, 2.5 mm
External I/O	USB I/F, Digitmatic Output, Printer Output, RS-232C I/F, Foot SW I/F

Table 3. Orthogonal array and response table.

Sl.No	A	B	C	Ra1	Ra2	Da1	Da2
1	1	1	2	4.93	4.186	75.09	127.66
2	2	3	3	4.399	5.512	110.236	154.01
3	2	1	3	4.345	3.506	115.664	115.833
4	2	3	2	4.892	5.609	66.252	138.52
5	2	2	2	5.079	4.832	89.232	73.957
6	3	2	2	4.379	4.592	99.104	72.66
7	2	3	1	5.369	5.592	51.661	88.22
8	2	2	3	4.652	4.372	129.006	140.56
9	2	1	2	4.125	3.972	61.88	72.06
10	1	2	1	5.154	5.486	43.99	56.192
11	2	2	1	5.339	5.259	65.158	46.709
12	1	1	1	5.115	4.195	50.12	66.737
13	1	2	2	4.879	4.779	99.859	125.678
14	3	2	3	4.725	3.892	109.627	93.921
15	3	1	2	4.105	4.292	80.48	121.293
16	1	2	3	4.812	5.139	105.45	122.06
17	2	2	1	5.285	4.521	46.458	68.47
18	3	3	1	4.327	5.752	65.44	51.032
19	1	3	1	5.105	5.186	65.001	66.596
20	1	1	3	4.184	3.434	123.26	103.322
21	1	3	2	5.98	6.332	77.86	97.725
22	2	1	1	4.545	3.732	87.468	84.074
23	3	3	3	4.259	5.772	112.225	123.928
24	3	3	2	4.91	5.286	82.327	112.04
25	3	1	1	4.072	4.692	51.253	56.395
26	3	1	3	3.372	4.219	124.496	77.843
27	1	3	3	4.836	4.772	96.446	105.95

There are two (k = 2) replications of the processes. The responses have varying ranges and are measured in various units. The normalization method brings the results of multi-response optimization into the range of 0 to 1. Normalization reduces the reactions to a range that is suitable for continued use.

3. Results and Analysis

3.1. ANOVA Analysis

The results of the analyses conducted on surface roughness and delamination can be found in Tables 4 and 5, respectively. ANOVA was carried out at a 95% confidence level. Table 4 confirms that the parameter standoff distance has a significant influence on the surface roughness produced, with an influence of 68.44%. This means that even a small variation in this parameter can cause a huge difference in the surface roughness. Therefore, it is not advisable to vary this parameter. The abrasive mass flow rate parameter has the next highest level of significance on surface roughness, with an influence of 6.70%. Since this parameter does not have a significant impact, it can be varied to some extent. The parameter traverse speed has the least significance on surface roughness at only 1.47%, so variation in this parameter will not make a huge difference in the output parameter. Therefore, this variable can be fixed at any value within the selected range according to the requirement.

Table 4. ANOVA table for surface roughness.

Source	DF	Seq SS	Adj SS	Adj Ms	F	P
TS	2	0.06565	0.06565	0.03283	0.36	0.0706
SOD	2	9.49434	9.49434	4.74717	52.58	0.000
MFR	2	0.93051	0.93051	0.46526	5.15	0.036
Error	8	0.72225	0.72225	0.09028		
Total	26	13.87097				

S = 0.300469, R-Sq = 94.79%, R-Sq(adj) = 83.08%.

Table 5. ANOVA table for delamination.

Source	DA	Seq SS	Adj SS	Adj MS	F	P
TS	1	64.51	64.52	64.51	0.721	0.406
SOD	1	248.61	248.62	248.61	2.741	0.112
MFR	1	15,338.7	15,338.7	15,338.7	168.49	0.000
Error	23	2092.91	2092.91	92.1		
Total	26	17,747.7				

S = 9.5413, R-Sq = 88.20%, R-Sq(adj) = 86.66.

Simultaneously, Table 5 displays the ANOVA for delamination that occurred during machining. From the table, it is clear that the abrasive mass flow rate is the most significant parameter affecting delamination, with a significance of 85%. The second most significant parameter is standoff distance, with a significance of 2%. The least significant parameter is traverse speed, with a significance of 0.5%. Therefore, traverse speed can be set to any desired value within the given range. ANOVA is a widely used method to predict the level of influence of input parameters on the output response. However, it has certain drawbacks. One such drawback is that the data need to be normally distributed for ANOVA to work accurately and reliably. If the data are not normally distributed, then the results obtained from ANOVA will not be accurate. This can be especially problematic while dealing with small samples, as it increases the likelihood of non-normally distributed data within them.

ANOVA is a statistical method that has certain assumptions, such as equal variance among groups and independence of observations across groups. However, these assumptions may not hold true when dealing with smaller sample sizes. To draw valid conclusions from ANOVA tests, it is important to meet these conditions. Failure to do so with smaller sample sizes can limit our ability to obtain reliable results from an analysis conducted via ANOVA methods.

3.2. Effect of Standoff Distance on Surface Roughness and Delamination

Experimental studies have shown that surface roughness is significantly affected by the standoff distance parameter. Longer standoff distances tend to increase surface roughness. This happens because the water jet expands before it touches the composite material, making it more prone to external drag from the environment. Therefore, to achieve a smoother surface, a smaller standoff distance is preferable. Increasing the abrasive flow rate leads to a higher number of cutting particles used in the cutting process. This results in a smoother cut surface, as the jet more easily penetrates the laminate. However, there is a certain point beyond which roughness increases as the mass flow rate of the abrasive increases. This happens because an increase in abrasive particle mass leads to inter-particle collisions, which in turn cause a loss of kinetic energy. Most of the time, a rise in surface roughness can be achieved by increasing the traverse speed. This is because when the traverse speed is lower a greater number of cutting particles are involved in the cutting process and are impinging on the same area. As a result, the material is cut by the initial impinging particles, and the material is smoothed by the subsequent impinging cutting particles, thus improving surface smoothness. Therefore, it is always preferable to choose a slower traverse speed [22,23].

It has been proven through experimentation that the rate of abrasive mass flow significantly impacts the occurrence of delamination. An increase in the mass flow rate of abrasive particles results in a higher level of damage. This is because an increase in the number of particles per unit volume leads to particle collisions during flow when the number exceeds the optimal value. This impact affects the motion of abrasive particles, resulting in turbulence. Turbulence causes the cutting jet to deviate more, which increases the damaged area. As the jet approaches the bottom surface, its cutting energy and velocity decrease due to an increase in standoff distance. Consequently, the bottom layers of the composites receive less impact force, resulting in cutting action instead of piercing or shearing. Therefore, pushdown delamination decreases while standoff distance escalates during the composite machining. However, there is an optimal value beyond which the jet diversion increases, leading to greater delamination. The cutting area per unit time is enhanced with the cutting speed, resulting in small cutting action and greater abrasive penetration into the composites. Hence, an increase in cutting speed leads to an increase in delamination [24,25].

4. Optimization Using Grey Relational Analysis

4.1. Normalization

Three categories of response parameters exist: maximally beneficial, minimally beneficial, and nominally beneficial. Any one of the following three responses is acceptable; the combination of all non-beneficial, or all beneficial is used here. In this paper, trial I, replication *k*, and non-beneficial attribute *j* all have identical responses.

The normalized response is:

$$\boldsymbol{\Delta_{ijk}} = \frac{X_{ijk} - MinX_{ijk}}{MaxX_{ijk} - MinX_{ijk}} \tag{1}$$

The normalized response $\boldsymbol{\Delta_{ijk}}$ ranges from 0 to 1.

4.2. Estimation of Grey Relational Coefficient GRC_{ijk}

The grey relational coefficient is estimated by the equation:

$$GRC_{ijk} = \frac{Min\Delta_{ijk} + \xi Max\Delta_{ijk}}{\Delta_{ijk} + \xi Max\Delta_{ijk}} \tag{2}$$

where ξ is the distinguishing coefficient ranging from 0 to 1. Normally, 0.5 is taken as the value of ξ, indicating that equal weightage is given to both the output responses. The estimated GRC_{ijk} is presented in Table 6.

Table 6. L_{27} Orthogonal Array with Grey Relational Coefficients (GRC_{ijk}).

Sl.No	A	B	C	Ra1	Ra2	Da1	Da2	Norm Ra1	Norm Ra2	Norm Da1	Norm Da2	GRC Ra1	GRC Ra2	GRC Da1	GRC Da2
1	1	1	2	4.93	4.186	75.09	127.66	0.597	0.259	0.366	0.754	0.456	0.658	0.577	0.399
2	2	3	3	4.399	5.512	110.236	154.01	0.394	0.717	0.779	1.000	0.559	0.411	0.391	0.333
3	2	1	3	4.345	3.506	115.664	115.833	0.373	0.025	0.843	0.644	0.573	0.953	0.372	0.437

Table 6. *Cont.*

Sl.No	A	B	C	Ra1	Ra2	Da1	Da2	Norm Ra1	Norm Ra2	Norm Da1	Norm Da2	GRC Ra1	GRC Ra2	GRC Da1	GRC Da2
4	2	3	2	4.892	5.609	66.252	138.52	0.583	0.751	0.262	0.856	0.462	0.400	0.656	0.369
5	2	2	2	5.079	4.832	89.232	73.957	0.655	0.482	0.532	0.254	0.433	0.509	0.484	0.663
6	3	2	2	4.379	4.592	99.104	72.66	0.386	0.400	0.648	0.242	0.564	0.556	0.435	0.674
7	2	3	1	5.369	5.592	51.661	88.22	0.766	0.745	0.090	0.387	0.395	0.402	0.847	0.564
8	2	2	3	4.652	4.372	129.006	140.56	0.491	0.324	1.000	0.875	0.505	0.607	0.333	0.364
9	2	1	2	4.125	3.972	61.88	72.06	0.289	0.186	0.210	0.236	0.634	0.729	0.704	0.679
10	1	2	1	5.154	5.486	43.99	56.192	0.683	0.708	0.000	0.088	0.423	0.414	1.000	0.850
11	2	2	1	5.339	5.259	65.158	46.709	0.754	0.630	0.249	0.000	0.399	0.443	0.668	1.000
12	1	1	1	5.115	4.195	50.12	66.737	0.668	0.263	0.072	0.187	0.428	0.656	0.874	0.728
13	1	2	2	4.879	4.779	99.859	125.678	0.578	0.464	0.657	0.736	0.464	0.519	0.432	0.405
14	3	2	3	4.725	3.892	109.627	93.921	0.519	0.158	0.772	0.440	0.491	0.760	0.393	0.532
15	3	1	2	4.105	4.292	80.48	121.293	0.281	0.296	0.429	0.695	0.640	0.628	0.538	0.418
16	1	2	3	4.812	5.139	105.45	122.06	0.552	0.588	0.723	0.702	0.475	0.459	0.409	0.416
17	2	2	1	5.285	4.521	46.458	68.47	0.734	0.375	0.029	0.203	0.405	0.571	0.945	0.711
18	3	3	1	4.327	5.752	65.44	51.032	0.366	0.800	0.252	0.040	0.577	0.385	0.665	0.925
19	1	3	1	5.105	5.186	65.001	66.596	0.664	0.605	0.247	0.185	0.429	0.453	0.669	0.730
20	1	1	3	4.184	3.434	123.26	103.322	0.311	0.000	0.932	0.528	0.616	1.000	0.349	0.487
21	1	3	2	5.98	6.332	77.86	97.725	1.000	1.000	0.398	0.475	0.333	0.333	0.557	0.513
22	2	1	1	4.545	3.732	87.468	84.074	0.450	0.103	0.511	0.348	0.526	0.829	0.494	0.589
23	3	3	3	4.259	5.772	112.225	123.928	0.340	0.807	0.803	0.720	0.595	0.383	0.384	0.410
24	3	3	2	4.91	5.286	82.327	112.04	0.590	0.639	0.451	0.609	0.459	0.439	0.526	0.451
25	3	1	1	4.072	4.692	51.253	56.395	0.268	0.434	0.085	0.090	0.651	0.535	0.854	0.847
26	3	1	3	3.372	4.219	124.496	77.843	0.000	0.271	0.947	0.290	1.000	0.649	0.346	0.633
27	1	3	3	4.836	4.772	96.446	105.95	0.561	0.462	0.617	0.552	0.471	0.520	0.448	0.475

4.3. Estimation of Grey Relational Grade GRG_i

The average of GRC in each row is known as Grey relational grade GRG_i. The Grey relational grade GRG_i is given by the formula:

$$GRC_i = \frac{\sum_1^m \sum_1^n GRC_{ijk}}{mn} \tag{3}$$

where m is the number of response parameters and n is the number of replications (n = 2). The orthogonal array and GRGi are shown in Table 7.

Table 7. Orthogonal array and GRGi.

Sl.No	A	B	C	GRG
1	1	1	2	0.523
2	2	3	3	0.424
3	2	1	3	0.584

Table 7. *Cont.*

Sl.No	A	B	C	GRG
4	2	3	2	0.472
5	2	2	2	0.522
6	3	2	2	0.557
7	2	3	1	0.552
8	2	2	3	0.452
9	2	1	2	0.687
10	1	2	1	0.672
11	2	2	1	0.627
12	1	1	1	0.671
13	1	2	2	0.455
14	3	2	3	0.544
15	3	1	2	0.556
16	1	2	3	0.440
17	2	2	1	0.658
18	3	3	1	0.638
19	1	3	1	0.570
20	1	1	3	0.613
21	1	3	2	0.434
22	2	1	1	0.690
23	3	3	3	0.443
24	3	3	2	0.469
25	3	1	1	0.722
26	3	1	3	0.657
27	1	3	3	0.478

4.4. Average GRG Estimation for Each Level

For every level, the average GRG is determined. The ideal value for that parameter is the level at which the GRG is maximal for each factor j. Table 8 lists the average GRG. Figure 3a–c displays the average GRG vs. parameters at various levels.

Table 8. Estimated average GRG with corresponding factors.

Factors	A	B	C
Level 1	0.530	**0.625**	**0.636**
Level 2	**0.583**	0.548	0.519
Level 3	0.553	0.498	0.515
Range	0.053	0.127	0.121
Rank	3	1	2

The range for each parameter is determined by the difference between the maximum average GRG and the minimum GRG. The most crucial component is the one with a wide range. The ranking is based on the average GRG.

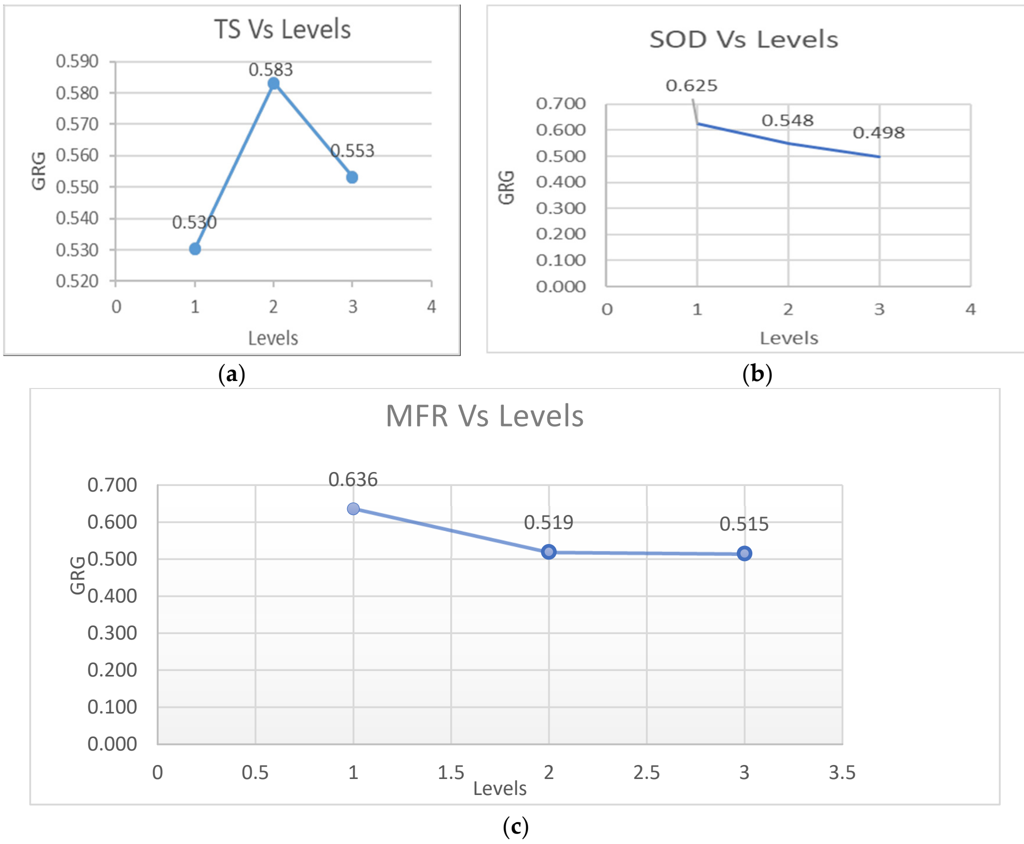

Figure 3. The average GRG vs. parameters at different levels. (**a**) GRG vs. TS, (**b**) GRG vs. SOD and (**c**) GRG vs. MFR.

4.5. Selection of Optimum Levels of Process Parameters

A setup that maximizes the average GRG for a certain factor is considered optimal. A2-B1-C1, or TS = 25 mm, SOD = 2 mm, and MFR = 0.25 kg/min, is the ideal configuration.

4.6. ANOVA Application to Identify the Influence of Each Parameter

ANOVA is used to reconfirm the ideal configuration, and Table 9 lists the sum of squares for each level. Table 10 displays the ANOVA table for GRG.

The unpooled ANOVA on GRG is computed using the above computations. Table 10 displays the calculated values.

The relevant factor is the one for which F computed > F table. Furthermore, by dividing each estimated value of F by the total calculated value of F, the percentage contribution for each factor is determined.

Table 9. The total GRG with their corresponding factors.

Factors	A	B	C
Level 1	4.772	5.622	5.720
Level 2	5.831	4.928	4.674
Level 3	4.425	4.479	4.634
Sum of squares SS factors	0.0134	0.074	0.084
Sum of squares Error SS error	0.042		

Table 10. Values of unpooled ANOVA upon GRG.

Factors	Sum of Squares	Degrees of Freedom (DOF)	Mean Sum of Squares (MSS)	F Calculated	F Table (5% Risk)	Remark	Percentage Contribution
A	0.0134	2	0.007	3.161	2.59	Significant	7.830
B	0.0735	2	0.037	17.330	2.59	Significant	42.933
C	0.084	2	0.042	19.874	2.59	Significant	49.236
Error	0.042	20	0.002				
Total	0.214	26					

4.7. Estimation of GRG Predicted

The GRG predicted is estimated utilizing the equation:
Let T = Overall average of Grey relational grades = Total GRG/27 = 0.557
The predicted GRG is given by $GRG_{predicted} = Average\ GRG\ for\ (A_2 + B_1 + C_1) - 2T$
The predicted GRG is given by $GRG_{predicted}$ = 0.730

4.8. Confidence Interval Estimation (C.I.)

The expected range of GRG for the ideal conditions is shown by the confidence interval. The confidence interval computation is displayed below.

Half width of confidence interval:

$$\sqrt{\frac{F_{\alpha(1,\ dof\ of\ error)} * MSS_{error}}{\eta_{eff}}} \tag{4}$$

where η_{eff} is the effective sample size.

The effective sample size:

$$\eta_{eff} = \frac{N}{(1 + Total\ of\ Dof\ of\ each\ factor)} = \frac{27}{07} = 3.857 \tag{5}$$

The $F_{\alpha(1,\ Dof\ of\ error)}$ is taken from F table. α = 95% (confidence level), DOF of error is 20.

$$F_{\alpha(1,\ Dof\ of\ error)} = F_{0.05(1,20)} = 4.35$$

$$\mathrm{d} = \sqrt{\frac{4.35 * 0.002}{3.857}} = 0.049$$

The following provides the anticipated mean's confidence interval at a 90% confidence level (C.I.): C.I. = Predicted average GRG ± d; 0.681 < C.I. < 0.779.

With the following optimal settings, a confirmation test was carried out for verification:

Traverse Speed = 25 mm/min,

Standoff distance = 2 mm,

MFR = 0.25% kg/min.

The confirmation test was conducted, and the corresponding GRG was found to be 0.690. This shows that the GRG predicted is acceptable. The minimum standoff distance (SOD) with minimum mass flow rate (MFR) ensures thorough mixing of abrasives with fluid. In addition, moderate traverse speed leads to an easy flow of abrasives and debris, resulting in minimum surface roughness and minimum delamination effect. Hence, these elements working together produce the best possible reaction. It is evident from the ranks of process factors that the standoff distance (rank 1) has the highest impact on the results. When it comes to regulating the reaction, SOD and MFR work better than traversal speed. When considering all factors, the optimal GRG value is 0.722 with settings A3-B1-C1. This setting allows for a faster traverse speed of 30 mm/min, resulting in a smoother water jet flow and a cleaner surface.

Grey relational analysis (GRA) is sensitive to the initial arrangement of data. Even small changes in the order of data can lead to different grey relational coefficients, which may affect the final ranking of alternatives. GRA requires the selection of certain parameters, such as the grey relational degree and the distinguishing coefficient. However, the choice of these parameters can be subjective and may impact the results. In fact, different analysts may choose different parameters, leading to varying outcomes. It is also important to note that GRA assumes a linear relationship between factors, which may not always be accurate in real-world scenarios. In cases where the relationship is nonlinear, GRA may not provide accurate results.

5. Conclusions

- The procedure for grey relational analysis is simple and does not require knowledge of computer software;
- This analysis is effective in handling cases with multiple output responses, even with contradictory objectives. In this paper, both responses have the same objective—the minimum is better;
- When there are a large number of parameters and levels, the Taguchi table is used to select parameters for trials. This table is designed to ensure that the result of any trial is not influenced by other trials, and to minimize the number of trials required;
- The ranking of parameters A, B, and C provides insight into which parameters need to be carefully controlled to achieve the desired output. The SOD is given a rank of 1, indicating that even a small variation in SOD can significantly impact the output of Ra and Da;
- The application of ANOVA to GRG proves that the results of the grey relational analysis are reliable. The confirmation test shows how reliable the forecasts are. The optimally configured GRG in this work falls within the confidence interval that represents the appropriate optimal configuration. The setting is within the confidence interval, depicting the proper optimal setting.

6. Scope for Future Work

The current study focuses on optimizing two output parameters, namely delamination and surface roughness, using a specific method. The aim of this method is to minimize both parameters simultaneously. Researchers working on the Abrasive Water Jet Machining (AWJM) process in the future could adopt this multiple response optimization technique to optimize more than two parameters. This particular approach can be used to minimize some responses and maximize others. For example, it can be used to minimize surface roughness and delamination while maximizing the material removal rate.

Author Contributions: Conceptualization and methodology, J.P.K.; software and validation, M.B.; formal analysis and investigation, R.B.; resources and data curation, S.R.P.; writing—original draft preparation, writing—review and editing, M.B.; visualization and supervision, M.B. All authors have read and agreed to the published version of the manuscript.

Funding: This research received no external funding.

Data Availability Statement: Data are contained within the article.

Conflicts of Interest: The authors declare no conflict of interest.

References

1. Mohit, H.; Mavinkere Rangappa, S.; Siengchin, S.; Gorbatyuk, S.; Manimaran, P.; Alka Kumari, C.; Khan, A.; Doddamani, M. A Comprehensive Review on Performance and Machinability of Plant Fiber Polymer Composites. *Polym. Compos.* **2022**, *43*, 608–623. [CrossRef]
2. Schwartzentruber, J.; Spelt, J.K.; Papini, M. Prediction of Surface Roughness in Abrasive Waterjet Trimming of Fiber Reinforced Polymer Composites. *Int. J. Mach. Tools Manuf.* **2017**, *122*, 1–17. [CrossRef]

3. Sabarinathan, P.; Annamalai, V.E.; Rajkumar, K. Optimization of Process Parameter in Abrasive Water Jet Machining of Blue-Fired Grain-Reinforced Glass Fiber Polymer Composite. In *Trends in Manufacturing and Engineering Management Select Proceedings of ICMechD 2019*; Springer: Singapore, 2021; pp. 217–226.
4. Armağan, M.; Arici, A.A. Cutting Performance of Glass-Vinyl Ester Composite by Abrasive Water Jet. *Mater. Manuf. Process.* **2017**, *32*, 1715–1722. [CrossRef]
5. Sisodia, V.; Gupta, S.K.; Salunkhe, S.; Murali, A.P.; Kumar, S. An Experimental Investigation on Machining of Hardened AISI 440C Stainless Steel Using Abrasive Water Jet Machining Process. *J. Mater. Eng. Perform.* **2023**, *1*, 1–17. [CrossRef]
6. Natarajan, Y.; Raj, K.L.N.; Tandon, P. Measurement and Analysis of Pocket Milling Features in Abrasive Water Jet Machining of Ti-6Al-4V Alloy. *Arch. Civ. Mech. Eng.* **2022**, *23*, 42. [CrossRef]
7. Wang, H.; Yuan, R.; Zhang, X.; Zai, P.; Deng, J. Research Progress in Abrasive Water Jet Processing Technology. *Micromachines* **2023**, *14*, 1526. [CrossRef]
8. Madival, A.S.; Doreswamy, D.; Shetty, R.; Naik, N.; Gurupur, P.R. Optimization and Prediction of Process Parameters during Abrasive Water Jet Machining of Hybrid Rice Straw and *Furcraea foetida* Fiber Reinforced Polymer Composite. *J. Compos. Sci.* **2023**, *7*, 189. [CrossRef]
9. Kavimani, V.; Gopal, P.M.; Sumesh, K.R.; Kumar, N.V. Multi Response Optimization on Machinability of SiC Waste Fillers Reinforced Polymer Matrix Composite Using Taguchi's Coupled Grey Relational Analysis. *Silicon* **2022**, *14*, 65–73. [CrossRef]
10. Thakur, R.K.; Singh, K.K. Experimental Investigation and Optimization of Abrasive Water Jet Machining Parameter on Multi-Walled Carbon Nanotube Doped Epoxy/Carbon Laminate. *Measurement* **2020**, *164*, 108093. [CrossRef]
11. Chenrayan, V.; Manivannan, C.; Shahapurkar, K.; Zewdu, G.A.; Maniselvam, N.; Alarifi, I.M.; Alblalaihid, K.; Tirth, V.; Algahtani, A. An Experimental and Empirical Assessment of Machining Damage of Hybrid Glass-Carbon FRP Composite during Abrasive Water Jet Machining. *J. Mater. Res. Technol.* **2022**, *19*, 1148–1161. [CrossRef]
12. Altin Karataş, M.; Motorcu, A.R.; Gökkaya, H. Study on Delamination Factor and Surface Roughness in Abrasive Water Jet Drilling of Carbon Fiber-Reinforced Polymer Composites with Different Fiber Orientation Angles. *J. Braz. Soc. Mech. Sci. Eng.* **2021**, *43*, 22. [CrossRef]
13. Gopal, P.M.; Kavimani, V.; Arunkumar, K. Multi-Objective Optimization on Abrasive Water Jet Machining of Epoxy/Glass Fiber/Grinding Wheel Particle Composite through Hybrid Optimization Technique. *Multiscale Multidiscip. Model. Exp. Des.* **2023**, *6*, 697–707. [CrossRef]
14. Szatkiewicz, T.; Perec, A.; Radomska-Zalas, A.; Banaszek, K.; Balasz, B. Preliminary Studies into Cutting of a Novel Two Component 3D-Printed Stainless Steel–Polymer Composite Material by Abrasive Water Jet. *Materials* **2023**, *16*, 1170. [CrossRef] [PubMed]
15. Perec, A.; Radomska-Zalas, A.; Fajdek-Bieda, A.; Pude, F. Process optimization by applying the response surface methodology (rsm) to the abrasive suspension water jet cutting of phenolic composites. *FACTA Univ. Ser. Mech. Eng.* **2022**, *1*, 575–589.
16. Perec, A.; Musial, W.; Prazmo, J.; Sobczak, R.; Radomska-Zalas, A.; Fajdek-Bieda, A.; Nagnajewicz, S.; Pude, F. Multi-criteria Optimization of the Abrasive Waterjet Cutting Process for the High-Strength and Wear-Resistant Steel Hardox®500. In *International Conference on Water Jet—Research, Development, Applications*; Springer: Cham, Switzerland, 2020; Volume 1, pp. 145–154.
17. Jiang, Y.; Yarin, A.L.; Pan, Y. Printable Highly Transparent Natural Fiber Composites. *Mater. Lett.* **2020**, *277*, 128290. [CrossRef]
18. Karim, N.; Sarker, F.; Afroj, S.; Zhang, M.; Potluri, P.; Novoselov, K.S. Sustainable and Multifunctional Composites of Graphene-Based Natural Jute Fibers. *Adv. Sustain. Syst.* **2021**, *5*, 2000228. [CrossRef]
19. Rangasamy, G.; Mani, S.; Kolandavelu, S.K.S.; Alsoufi, M.S.; Ibrahim, A.M.M.; Muthusamy, S.; Panchal, H.; Sadasivuni, K.K.; Elsheikh, A.H. An Extensive Analysis of Mechanical, Thermal and Physical Properties of Jute Fiber Composites with Different Fiber Orientations. *Case Stud. Therm. Eng.* **2021**, *28*, 101612. [CrossRef]
20. Yu, T.; Tuerhongjiang, T.; Sheng, C.; Li, Y. Phosphorus-Containing Diacid and Its Application in Jute/Poly (Lactic Acid) Composites: Mechanical, Thermal and Flammability Properties. *Compos. Part A Appl. Sci. Manuf.* **2017**, *97*, 60–66. [CrossRef]
21. Kalirasu, S.; Rajani, N.; Rajesh, S.; Gopikumar, S.; Arunkumar, K.; Mukesh Vaidya, C.M. Surface Quality of Jute Fibre Reinforced Epoxy Composite by Abrasive Waterjet Machining. *Int. J. Recent Technol. Eng.* **2019**, *8*, 196–199.
22. Ramakrishnan, S. Investigating the effects of abrasive water jet machining parameters on surface integrity, chemical state in machining of Ti-6Al-4V. *Mater. Today Commun.* **2022**, *31*, 1–9. [CrossRef]
23. Ramesha, K.; Santhosh, N.; Kiran, K.; Manjunath, N.; Naresh, H. Effect of the Process Parameters on Machining of GFRP Composites for Different Conditions of Abrasive Water Suspension Jet Machining. *Arab. J. Sci. Eng.* **2019**, *44*, 7933–7943. [CrossRef]
24. Manivannan, J.; Rajesh, S.; Mayandi, K.; Rajini, N.; Ayrilmis, N. Investigation of abrasive water jet machining parameters on turkey fibre reinforced polyester composites. *Mater. Today Proc.* **2021**, *45*, 8000–8005. [CrossRef]
25. Sumesh, K.R.; Kanthavel, K. Abrasive Water Jet Machining of Sisal/Pineapple Epoxy Hybrid Composites with the Addition of Various Fly ash Filler. *Mater. Res. Express* **2020**, *7*, 035303. [CrossRef]